OPTIMUM DESIGN OF THE MAGNETIC BEARING-CONTROLLED ROTOR SYSTEM

An-Chen Lee
Foam-Zone Hsiao
Department of Mechanical Engineering
National Chiao Tung University
Hsinchu, Taiwan, R.O.C.

ABSTRACT

This paper proposes a design method which synthesizes the optimum design of the rotor structure, the control system, and the magnetic bearing simultaneously. We first derive the model of the electromagnetic bearing-controlled rotor system. A criterion based on minimizing the rotor response and the control current is then used to seek the optimum bearing dimensions. This criterion needs to solve the Riccati equation. The constraint on the peak rotor time response, the control current, and the flux density of the bearing's stator are included in this study. Sensitivity analysis of both the cost function and the constraints are also described. Numerical analysis shows the effect of different weightings and the superiority of this design methodology.

NOMENCLATURE

A_g	effective cross section area of air gap
B_{sat}	saturation magnetic flux density of core material
D_{max}	the maximum allowable diameter of the stator.
D_s	outer diameter of the stator
d_{mb}, t_{mb}	diameter and thickness of disks #1, #2
d_n	displacement of rotor at location of electromagnet n, n=1~8
$\boldsymbol{F_d}$	impulse loading
$\boldsymbol{F_u}$	unbalance loading
$\boldsymbol{F_1}$~$\boldsymbol{F_8}$	electromagnetic forces
G	size of air gap
h, s, W_m	dimensions of the bearing's pole piece
I_b	bias current
I_u	maximum available current provided by the current driver
i_n	control current corresponding to electromagnet n, n=1~8
$\boldsymbol{K}$	optimal feedback gain matrix
L_1~L_3	locations of the disks #1, #2, and #3
$\boldsymbol{M}, \boldsymbol{C}, \boldsymbol{S}$	inertia, damping, and stiffness matrices
N	turns of coil winding around a pole
$\boldsymbol{Q}, \boldsymbol{R}$	weighting matrices for state and input
x_3, y_3	displacement of rotor disk #3
α	half of the span angle between the two pole ribs of an electromagnet
γ_1	ratio of maximum rotor deviation to the air gap size
ξ	design variable
μ_0	permeability of free space, 4π*1.0e—7
ω	rotating speed of the rotor

Superscript and Subscript

$(\cdot)^t$	transpose
$(\cdot)_{,\xi}$	derivative with respect to ξ

INTRODUCTION

Magnetic bearings are newly-risen field interesting researchers majoring in electric and mechanic engineering. For most of the applications, the needs of low vibration and large load capacity are two major targets pursued by the magnetic bearing designers.

A large part of papers focus the issue on the design of controllers; they take the magnetic bearing as an actuator with known properties, and then try to seek the appropriate controller [1—3]. Another part of papers investigate the bearing

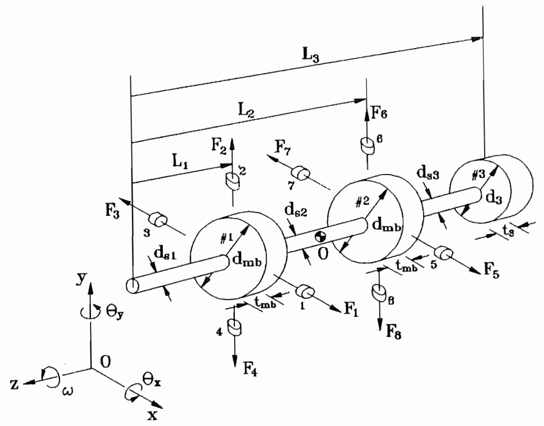

FIGURE 1: The Rotor-Bearing System

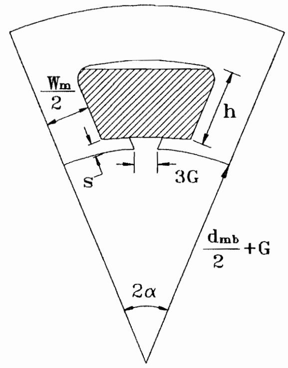

FIGURE 2: Dimension of the Magnetic Pole Piece

characteristics [4,5]. However, a successful design of the magnetic-bearing-suspended rotor system relies on both the bearing itself and the controller. Thus, we synthesize the optimum design of the rotor structure, the control system, and the magnetic bearing simultaneously. Based on such a methodology, we can get designs that contain less mass and use less control effort than those achieved by iterating between structural and control synthesis. Also we can handle the cross-coupling effects and dynamic interactions between the structures and the control systems.

The system analyzed here is shown in Fig. 1. Because of the misalignment during assembling process or the key of the rotor shaft, unbalance load usually exists when the rotor is rotating. In addition, a rotor system immune from impulse disturbance or capable of quickly return to its central position is highly desirable. A good magnetic bearing suspended rotor system is thus capable of minimizing the effect of unbalance loading and impulse disturbance with as small control effort as possible. So we try to seek the most proper dimensions and locations of the magnetic bearings to reach the objectives mentioned above.

SYSTEM MODELING

The magnetic bearing force is obtained by providing a large bias current to each coil winding and a regulating current accommodating the rotor displacement to the corresponding coil winding. By assuming no flux leakage and neglecting the reluctance of soft iron and the phenomenon of fringing effect, we express the magnetic force as a nonlinear function of coil current and gap length, as follows:

$$F_n = \frac{\mu_0 A_g N^2 (I_b + i_n)^2 \cos\alpha}{(G - d_n \cdot \cos\alpha)^2}, \quad n = 1 \sim 8 \quad (1)$$

In Eq. (1), the number of turns of the coil windings N and the effective cross section area of the air gap A_g are two quantities that should be related to the design variables. Figure 2 shows the effective slot space in our design (the hatched region); the dimensions of the magnetic bearing are also shown here. By experience, the most effective winding space is about eighty percent of the effective slot space in which the copper wire can be arranged tightly. We can approximate the most effective winding space as a trapezoid region, which we express as follows:

$$A_w = 0.8[(d_{mb} + 2G + 2s + h)\sin\alpha - W_m \cos\alpha] \cdot h \cdot \cos\alpha \quad (2)$$

Thus N can be obtained from dividing A_w by the cross section area of the copper wire A_{coil}, i.e.,

$$N = 0.5 A_w / A_{coil} \quad (3)$$

Evaluation of A_g can be obtained by

$$A_g = c \cdot t_{mb} \cdot W_m \quad (4)$$

where the factor c is the ratio of A_g to the minimum cross section area of the pole piece (c is taken as 1.2 in this study).

In the control circuit, we let the control currents of the eighth electromagnets satisfy the following relations:

$$i_3 = -i_1, \qquad i_4 = -i_2$$
$$i_7 = -i_5, \qquad i_8 = -i_6 \quad (5)$$

To provide a magnetic force balancing the rotor's weight, we let the vertical direction coils carry additional part of static control current, that is

$$i_2 = \bar{i}_2 + i_{20}, \qquad i_6 = \bar{i}_6 + i_{60} \quad (6)$$

To simplify the analysis, we let the two magnetic bearings have the same dimensions and the same characteristics. Also we assume the rotor as a rigid body. By linearizing the bearing force equation and deriving the equation of motion in the transverse direction for the mass center of the rotor system, with these equations expressed in terms of the displacements at bearing's locations, we have

$$\boldsymbol{M}\ddot{\boldsymbol{Y}} + \boldsymbol{C}\dot{\boldsymbol{Y}} + \boldsymbol{S}\boldsymbol{Y} = \tilde{\boldsymbol{B}}\boldsymbol{U} \quad (7)$$

where

$$\boldsymbol{Y} = [d_1\ d_2\ d_5\ d_6]^t, \qquad \boldsymbol{U} = [i_1\ \bar{i}_2\ i_5\ \bar{i}_6]^t$$

The inertia matrix $\boldsymbol{M}$, damping matrix $\boldsymbol{C}$, and stiffness matrix $\boldsymbol{S}$ are all functions of the design variables. Matrix $\boldsymbol{C}$ is also a function of the rotor's rotating speed.

Representing Eq. (7) in state equation form, we have

$$\dot{\boldsymbol{X}} = \boldsymbol{A}\,\boldsymbol{X} + \boldsymbol{B}\,\boldsymbol{U} \tag{8}$$

where

$$\boldsymbol{A} = \begin{bmatrix} \boldsymbol{0} & \boldsymbol{I} \\ -\boldsymbol{M}^{-1}\boldsymbol{S} & -\boldsymbol{M}^{-1}\boldsymbol{C} \end{bmatrix}$$

$$\boldsymbol{B} = \begin{bmatrix} \boldsymbol{0} \\ \boldsymbol{M}^{-1}\tilde{\boldsymbol{B}} \end{bmatrix} \qquad \boldsymbol{X} = \begin{bmatrix} \boldsymbol{Y} \\ \dot{\boldsymbol{Y}} \end{bmatrix}$$

OPTIMAL CONTROLLER

A quadratic performance index based on the compromise of the magnitude of both the system state and the control effort is used in the optimal regulator theory. It is

$$J_{\mathrm{p}} = \int_0^{\infty} (\boldsymbol{X}^{\mathrm{t}}\boldsymbol{Q}\boldsymbol{X} + \boldsymbol{U}^{\mathrm{t}}\boldsymbol{R}\boldsymbol{U})\, \mathrm{d}t \tag{9}$$

where $\boldsymbol{Q}$ and $\boldsymbol{R}$ are weighting matrices. The matrix $\boldsymbol{Q}$ must be symmetric and positive semidefinite; the matrix $\boldsymbol{R}$ must be symmetric and positive definite. The optimal state feedback control which minimizes the quadratic performance index, while satisfying the state Eq. (8), is

$$\overset{*}{\boldsymbol{U}}(t) = -\,\boldsymbol{K}\cdot\overset{*}{\boldsymbol{X}}(t) \tag{10}$$

where $\overset{*}{\boldsymbol{U}}(t)$ is the optimal control input and $\overset{*}{\boldsymbol{X}}(t)$ is the corresponding state. The feedback gain matrix $\boldsymbol{K}$ is given by

$$\boldsymbol{K} = \boldsymbol{R}^{-1}\boldsymbol{B}^{\mathrm{t}}\boldsymbol{P} \tag{11}$$

where matrix $\boldsymbol{P}$ is the solution of the algebraic Riccati equation

$$\boldsymbol{Q} - \boldsymbol{P}\boldsymbol{B}\boldsymbol{R}^{-1}\boldsymbol{B}^{\mathrm{t}}\boldsymbol{P} + \boldsymbol{P}\boldsymbol{A} + \boldsymbol{A}^{\mathrm{t}}\boldsymbol{P} = \boldsymbol{0} \tag{12}$$

and $\boldsymbol{P}$ is a symmetric positive semidefinite matrix. When the optimal feedback control is adopted, the resulted closed loop system is asymptotically stable.

WEIGHTING MATRICES

Selection of weighting matrices $\boldsymbol{Q}$ and $\boldsymbol{R}$ is arbitrary except that the requirement of positive definiteness must be satisfied. Two common ways of selecting $\boldsymbol{Q}$ and $\boldsymbol{R}$ used in optimal control are

[Choice I]

$$\boldsymbol{Q} = \begin{bmatrix} q_1 & & 0 \\ & \ddots & \\ 0 & & q_{2n} \end{bmatrix} \qquad \boldsymbol{R} = \delta\cdot\boldsymbol{I} \tag{13}$$

[Choice II]

$$\boldsymbol{Q} = \begin{bmatrix} q_1\boldsymbol{S} & \boldsymbol{0} \\ \boldsymbol{0} & q_2\boldsymbol{M} \end{bmatrix}, \qquad \boldsymbol{R} = \delta\cdot\boldsymbol{I} \tag{14}$$

where q_i, i=1,$\cdots$,2n, and δ are scaling parameters that can be adjusted to control the amplitude of the dynamic response, the settling time, and the amplitude of the control current. In choice I, we minimize the weighted sum of the control effort and the rotor's vibrations; where we assume that the energy supplied to the rotor-bearing system is proportional to the control current and the influence of vibrations is evaluated by the squares of the rotor's displacement and velocity. In choice II, we minimize the weighted sum of the control effort, the system's potential energy, and the system's kinetic energy. However, because the stiffness matrix $\boldsymbol{S}$ is not positive definite (the uncontrolled rotor-bearing system has a negative spring constant), the requirement that $\boldsymbol{Q}$ must be at least semipositive definite is violated. Thus we adopt the choice I in the following analysis.

SYSTEM RESPONSES

In practical rotor-bearing systems, the occurrence of mass unbalance is usually unavoidable, and its effect should be considered especially at high rotating speeds. In our problem, we assume that the mass unbalance of the disks #1 and #2 used by the two magnetic bearings and the rotor disk #3 are located at a distance of e_1, e_2, and e_3, respectively, from their geometric center. The corresponding state equation is

$$\dot{\boldsymbol{X}} = \boldsymbol{A}\boldsymbol{X} + \boldsymbol{B}\boldsymbol{U} + \boldsymbol{F}_{\mathbf{u}} \tag{15}$$

where $\boldsymbol{F}_{\mathbf{u}}$ is the unbalance load vector acting on the center of gravity of the rotor-bearing system. Generally $\boldsymbol{F}_{\mathbf{u}}$ consists of both the force and the moment, and $\boldsymbol{F}_{\mathbf{u}}$ is dependent on both the structure variables and the locations of the magnetic bearings. Because the unbalance loading is closely related to the rotating speed, $\boldsymbol{F}_{\mathbf{u}}$ is also function of ω. In this study, we assume that the unbalance loading caused by the mass unbalance of the two magnetic bearings and by that of the rotor disk are in phase. Because $\boldsymbol{F}_{\mathbf{u}}$ is in sinusoidal waveform with frequency ω, we can express $\boldsymbol{F}_{\mathbf{u}}$ in complex form:

$$\boldsymbol{F}_{\mathbf{u}} = \mathrm{Re}(\boldsymbol{F}_{\mathbf{s}}\mathrm{e}^{\mathrm{j}\omega t}) \tag{16}$$

Because the x and y components of the unbalance force are in cosine and sine form, respectively, $\boldsymbol{F}_{\mathbf{s}}$ is a complex vector. Using the linear feedback control rule obtained from Eq. (10), the steady state solution of Eq. (15), $\boldsymbol{X}_{\mathbf{ss}}$, can be expressed as

$$X_{ss} = \mathrm{Re}(X_s e^{j\omega t}) \tag{17}$$

From Eqs. (15)~(17), we have

$$X_s = (j\omega I - A_c)^{-1} F_s \tag{18}$$

where

$$A_c = A - B \cdot K.$$

The time response of the unbalance/impulse loading can be obtained by directly solving the closed loop state equation

$$\dot{X} = A_c X + F \tag{19}$$

where for the case of impulse loading, $F=F_d$, while for the case of unbalance loading, $F=F_u$. In both cases, zero initial condition is used here.

OPTIMIZATION PROBLEM

Cost Function

The main objective of this study is to minimize the displacement of the rotor disk #3 when impulse loading or unbalance loading exist. In the case of impulse loading, we evaluate the maximum rotor displacement. In the case of unbalance loading, we evaluate the steady state response. We then seek a set of design variables $\mathbb{D}$ and an optimal control input U, so that the maximum deviation of the rotor disk #3 is minimized. Thus, the cost function is defined as

$$J = \min_{\mathbb{D}, U} \left(\max \left(x_3^2 + y_3^2\right)^{1/2}\right) \tag{20}$$

Constraint

In the practical design of an electromagnetic bearing, we encounter a number of restrictions due to the peripheral equipment or the bearing itself. These restrictions interfere with one another; for example, we may require larger load capacity, but the flux density will be saturated if the number of ampere-turns is too large. Therefore, we must find a compromise between these design constraints. The constraints used in this paper are listed as below:

(1) Flux density constraint

$$B_{max} \leq B_{sat} \tag{21}$$

(2) Coil current constraint

$$I_{max} \leq I_u \ (= 6 \text{ A}) \tag{22}$$

(3) Peak time response constraint

$$X_{max} \leq \gamma_1 G \tag{23}$$

(4) Maximum diameter of stator constraint

$$D_s \leq D_{max}$$

$$D_s = d_{mb} + 2G + 2(s + h + 1.1 W_m) \tag{24}$$

(5) Pole width constraint

$$W_m \leq [(0.5 d_{mb} + G) \cdot \sin\alpha - 1.5 G \cdot \cos\alpha] / 0.6 \tag{25}$$

(6) Constraint for the locations of the two magnetic bearings

$$L_1 < L_2 \tag{26}$$

Constraints for the diameters of the rotor shaft

(7) $d_{s1} \leq d_{mb}$

(8) $d_{s2} \leq d_{mb}$

(9) $d_{s3} \leq d_{mb}$ (27)

Sensitivity Analysis

Sensitivity analysis is necessary to obtain the solution of the optimization problem. Sensitivity of the cost function is evaluated by taking the derivative of Eq. (20) with respect to the design variable ξ, i.e.,

$$J_{,\xi} = \frac{dJ}{d\xi} \tag{28}$$

To get the sensitivity of cost function, we need to evaluate the sensitivity of the optimal feedback gain, which is obtained by evaluating the derivative of Eq. (11):

$$K_{,\xi} = R^{-1} B^t_{,\xi} P + R^{-1} B^t P_{,\xi} - R^{-1} R_{,\xi} R^{-1} B^t P \tag{29}$$

$$P_{,\xi} \bar{A} + \bar{A}^t P_{,\xi} + \bar{R} = 0 \tag{30}$$

in which

$$\bar{A} = A - B R^{-1} B^t P$$

$$\bar{R} = Q_{,\xi} + P A_{,\xi} + A^t_{,\xi} P - P (B R^{-1} B^t)_{,\xi} P$$

The sensitivity of constraints (4)~(9) in previous section is obvious and thus is omitted here. To obtain the sensitivity of the constraints (1)~(3), we need to compute the sensitivity of both the time response and the control input current. The time response sensitivity is evaluated by taking the derivative of the Eq. (19). Note that we just need to compute $X_{,\xi}$ at the specified time of occurrence of B_{max}, I_{max}, and X_{max}, respectively. The sensitivity of the control input is given by (using Eq. (10))

$$\overset{*}{U}_{,\xi} = -K_{,\xi} \overset{*}{X} - K \cdot \overset{*}{X}_{,\xi} \tag{31}$$

Thus we get all the required sensitivity information.

NUMERICAL ANALYSIS

Table 1 shows the design variables and the design data assigned to the rotor-bearing system. In the following analysis, we let the scaling parameters of the weighting matrix Q have the same value, i.e., $q_1 = q_2 = \ldots = q$. The optimization program MOST [6] is used to seek the solution and the MATLAB software is used to solve the Riccati equation and the time response. All the analysis is implemented on a 486 PC. For the optimization problem discussed previously, we have one cost

TABLE 1: Design variables and design data

design variable		upper−bound	lower−bound
d_{mb}	(m)	0.030	0.080
L_1	(m)	0.030	0.175
L_2	(m)	0.185	0.320
t_{mb}	(m)	0.005	0.030
W_m	(m)	0.010	0.030
h	(m)	0.005	0.060
d_{s1}	(m)	0.010	0.025
d_{s2}	(m)	0.010	0.025
d_{s3}	(m)	0.010	0.025
design data			**value**
D_{max}	(m)		0.14
B_{sat}	(tesla)		1.2
d_3	(m)		0.06
L_3	(m)		0.36
t_3	(m)		0.02
s	(m)		0.0015
α	(degree)		22.5
G	(m)		0.0008
I_b	(A)		1.2
A_{coil}	(m^2)		2.82743e−7
I_u	(A)		6.0
ω	(rpm)		10000
γ_1			0.2

function, nine constraints, and nine design variables.

There are fourteen cases investigated here. Cases 1—7 investigate the impulse loading condition, and cases 8—14 investigate the unbalance loading condition. Because of the page limitation, we only show the results of cases 1—3 and cases 8—10. In cases of impulse loading, the rotor disk #3 is subjected to a x-direction impulse load f_{xd}. Cases 1—3 investigate the effect of different set of scaling parameters q and δ on the optimum design. We conclude that a larger ration of q/δ causes a smaller optimal cost. The time histo ry of the displacement of rotor disk #3 and the control currents i_1, i_2, i_5, and i_6 for cases 1—3 are shown in Fig. 3. It can be seen that a larger ratio of q/δ causes a smaller peak rotor displacement. However, a larger ratio of q/δ causes a time delay for the rotor to return to the central position and the corresponding peak control currents are usually larger than in cases of smaller q/δ, which may be unavailable for practical implementation. Note that the currents $\bar{i}_2$ and $\bar{i}_6$ are non-zero because the gain matrix $\boldsymbol{K}$ is a full matrix, that is, the control in x and y directions are coupled. Thus y-

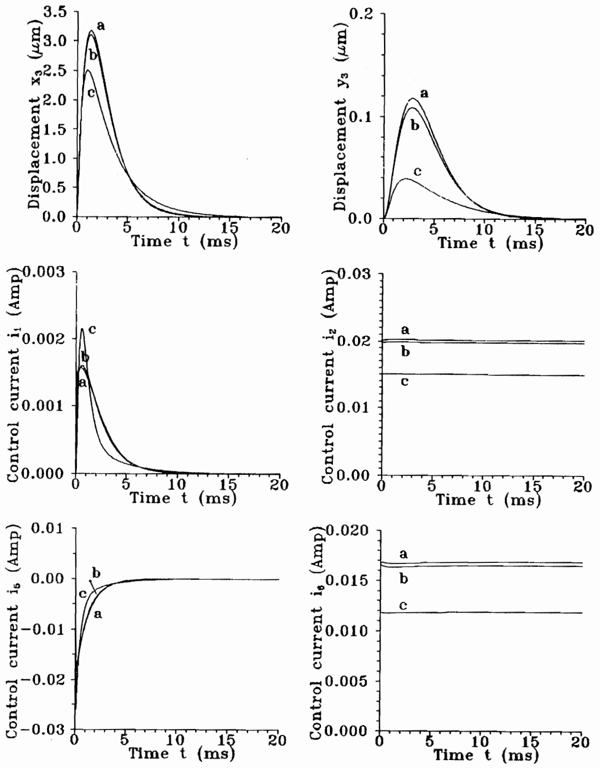

FIGURE 3: Time History (curve a:case1, q=1, δ=10; b:case2, q=1, δ=1; c:case3, q=10, δ=1)

direction rotor displacement appears though the system is subjected to x-direction impulse load only. The induced y-direction rotor displacement and the corresponding control current are smaller when a large ratio of q/δ is used. Note that, this induced displacement is small compared with the principle direction (x-direction) rotor displacement, and thus the induced displacement is of little significance. To see the merit of current optimum design, we further investigate three cases, in which the additional constraint for specific shaft diameters, bearing locations, and bearing dimensions are imposed on case 4, 5, and 6, respectively. Compare these result with the current optimum design (case2), we can verify the superiority of the current optimization method: the current design has smaller cost, quick time response, and smaller control current. The effect of different magnitude of impulse loading is investigated in case 7. As is expected, we need a larger bearing to accommodate the larger impulse loading. The final design for all cases show a similar trend in the final design structure, where we see the best use of the bearing dimensions and locations.

For cases of unbalance loading, we let the misalignment of the disk #1, #2, and #3 satisfy the specified ratio 1:1:2. Cases 8, 9, and 10 indicate that a larger value of the ratio q/δ causes a

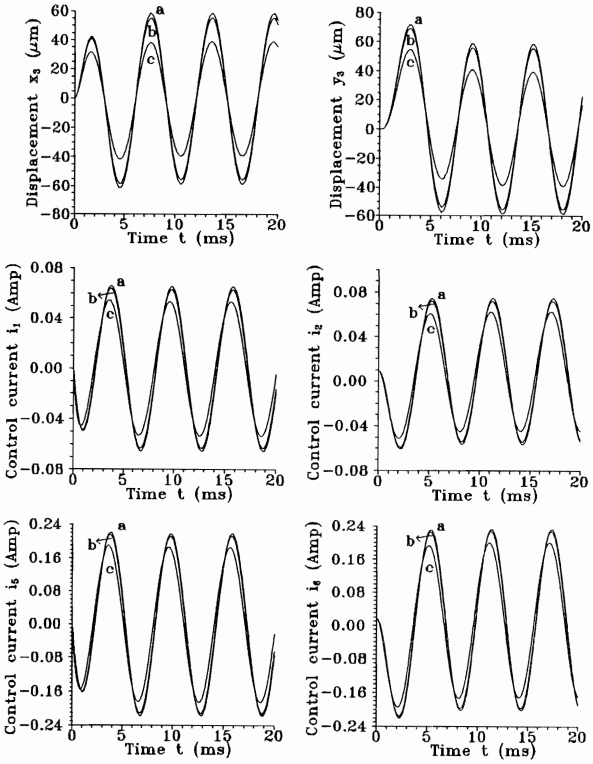

FIGURE 4: Time History (curve a:case8, q=1, δ=10; b:case9, q=1, δ=1; c:case10, q=10, δ=1)

smaller optimal cost. The corresponding time history of the rotor displacement and the control currents shown in Fig. 4 also demonstrate the preference of choosing a larger q/δ. However, the cases of impulse loading show that a larger q/δ causes a larger peak control current and a longer time delay. There should be a compromise for choosing q and δ. We also compare the time history for cases of the current optimum design (case 10), the specified shaft, the specified bearing locations, and the specified bearing dimensions. As is the same conclusion for cases of impulse loading, the results also demonstrate the superiority of the current optimization method. By investigating the effect of different magnitude of unbalance loading, we conclude that a larger size of magnetic bearing is also needed to accommodate the larger unbalance loading.

Experience in seeking the optimal solution for cases of impulse or unbalance loading indicates that the constraints on flux density and peak time response are active most frequently. For cases of larger loading, the maximum diameter of stator constraint is active sometimes.

CONCLUSION

A three-disk rotor-bearing system is illustrated for this integrated optimal design method. By using this method, we find a rotor-bearing system that is capable of minimizing the effect of unbalance loading and impulse disturbance with as small control effort as possible.

Numerical result demonstrates the superiority of this method. Analysis shows that a larger q/δ is preferred for a better unbalance loading response but a compromise in choosing q and δ is needed for the disturbance loading response. This analysis method can be extended to flexible rotor systems via incorporating the finite element method.

ACKNOWLEDGEMENTS

This study was sponsored by the National Science Council, Republic of China, under contract number NSC 81—0401—E—009—08.

REFERENCES

1. Matsumura, F. and Kobayashi, H., "Fundamental Equation for Horizontal Shaft Magnetic Bearing and Its Control System Design," Elec. Eng. in Japan, Vol. 101, No. 3, pp. 123—130, 1981.
2. Reinig, K.D. and Desrochers, A.A., "Disturbance Accommodating Controllers for Rotating Mechanical Systems," Trans. ASME, J. of Dynamic Systems, Measurement, and Control, Vol. 108, March, pp. 24—31, 1986.
3. Bradfield, C.D., Roberts, J.B. and Karunendiran, S., "A Programmable Electromagnetic Bearing for Vibration Control of a Flexible Shaft," ASME Trans., J. of Vib. and Acoustics., Vol. 113, April, pp. 160—166, 1991.
4. Maslen, E., Hermann, P., Scott, M. and Humphris, R.R., "Practical Limits to the Performance of Magnetic Bearings: Peak Force, Slew Rate, and Displacement Sensitivity," J. of Trib., Vol. 111, April, pp. 331—336, 1989.
5. Bornstein, K.R., "Dynamic Load Capabilities of Active Electromagnetic Bearings," J. of Trib., Trans. ASME, Vol. 113, July, pp. 598—603, 1991.
6. Tseng, C.H. and Lu, T.W., "Minimax Multiobjective Optimization in Structural Design," Int. J. for Numerical Methods in Eng., Vol. 30, pp. 1213—1228, 1990.